Medical Imaging
MVA 2024-2025

http://www-sop.inria.fr/teams/asclepios/cours/MVA/

X. Pennec

Analysis in the space of Covariance Matrices

Epione team
2004, route des Lucioles B.P. 93
06902 Sophia Antipolis Cedex

http://www-sop.inria.fr/epione

Medical Image Analysis – MVA 2024-2025

Course notes : http://www-sop.inria.fr/teams/asclepios/cours/MVA/

- Tue. Oct 1 2024, 14:00 ENS 1Z25 [XP] Introduction to Medical Image Acquisition & Image Registration
- Tue. Oct 8 2024, 14:00 ENS 1Z25 [XP] Riemannian Geometry and Statistics
- Tue. Oct 15 2024, 14:00 ENS 1Z25 [HD] Image Filtering & Segmentation
- Tue. Oct 22 2024: 14:00 ENS 1Z25 [HD] Image Segmentation based on Clustering and Markov Random Fields
- **Tue. Nov 5 2024: 14:00 ENS 1Z25 [XP] Analysis in the space of Covariance Matrices**
- Tue. Nov 12 2024: 14:00 ENS 1Z25 [HD] Shape constrained image segmentation
- Tue. Nov 19 2024: 14:00 ENS 1Z25 [XP] Diffeomorphic Registration and Computational Anatomy
- Tue. Nov 26 2024: 14:00 ENS 1Z25 [HD] Biophysical Modeling
- Tue. Dec 3, 2024, 14:00 (Visio) [XP & HD] Exam

Course overview

Computing with tensor images
- Diffusion tensor imaging
- Statistical computing on manifolds
- An affine invariant Riemannian metric
- Interpolation, filtering, diffusion PDEs on Tensors
- Other metrics

Applications of manifold valued image processing
- Diffusion tensor imaging
- Morphometry of sulcal lines on the brain

Introduction to diffusion tensor imaging (DTI)

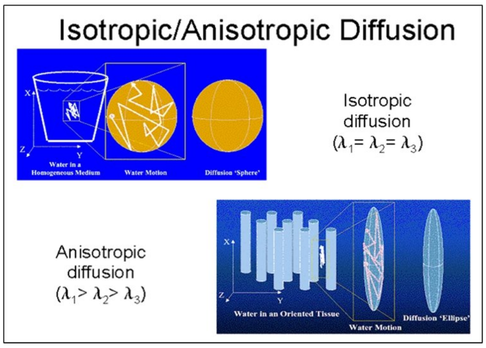

Introduction to diffusion tensor imaging (DTI)

Classical MRI:

- white mater, grey matter, CSF

Diffusion MRI:

- MR technique born in the mid-80ies (Basser, LeBihan).
- in vivo imaging of the white mater architecture
- set of nervous fibers (axons): information highways of the brain!

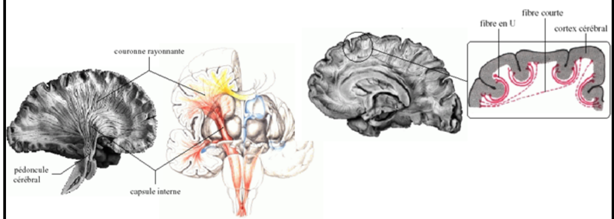

The Tenseur model

Mathematical definition:

- A multilinear application (generalization of matrices in linear algebra).

In medical imaging: real positive definite symmetric matrix

- All eigenvalues λ_i are real and positive (>0)
- Quadratic form = ellipsoid ($x^t \, \Sigma \, x = 1$)

$$\Sigma = \begin{bmatrix} \sigma_{11} & \sigma_{12} & \sigma_{13} \\ \sigma_{12} & \sigma_{22} & \sigma_{23} \\ \sigma_{13} & \sigma_{23} & \sigma_{33} \end{bmatrix} = V \, Diag(\lambda^2) V^t$$

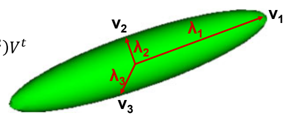

Stejskal & Tanner equation

Signal attenuation related to tensor using:

$$S_i = S_0 \, exp(-b.\vec{g_i}^t.D.\vec{g_i})$$

- S_i: diffusion weighted images;
- S_0: T2 image;
- g_i: spatial direction of the diffusion gradient;
- b: b-value (related to physical parameters of the acquisition, including field strength and diffusion time);
- D: diffusion tensor;

https://www.youtube.com/watch?v=J_aamnpRJE8

Anatomy of a diffusion MRI

T2 image

+

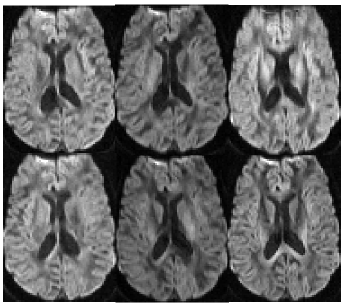

6 diffusion weighted images

Visualization using ellipsoids

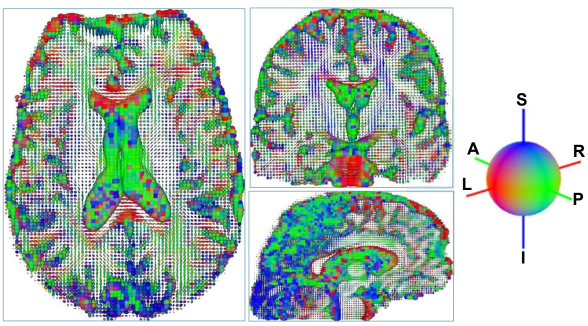

The Tensor Space is not a Vector Space

Tensors = Cone of positive definite matrices

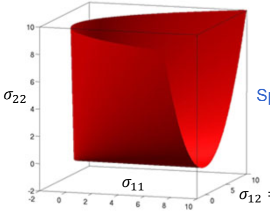

Matrices with null eigenvalues are reachable in a finite time

- Null and negatives eigenvalues are not physical

Intrinsic computing on Manifold-valued images?

Diffusion Tensor Imaging

Covariance of the Brownian motion of water
-> Architecture of axonal fibers

Symmetric positive definite matrices

- Cone: Convex operations are stable
  - mean, interpolation
  - Null eigenvalues are reachable in a finite time : not physical!
- More complex operations are not
  - PDEs, gradient descent…

SPD-valued image processing

- Clinical images: Very noisy data
- Robust estimation
- Filtering, regularization
- Interpolation / extrapolation

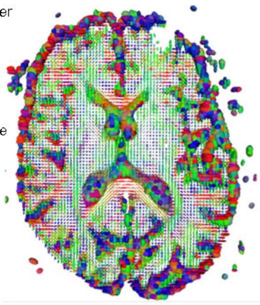

Diffusion Tensor Field
(slice of a 3D volume)

Intrinsic computing on Manifold-valued images?

Course overview

Computing with tensor images

- Diffusion tensor imaging
- Statistical computing on manifolds
- An affine invariant Riemannian metric
- Interpolation, filtering, diffusion PDEs on Tensors
- Other metrics

Applications of manifold valued image processing

- Diffusion tensor imaging
- Morphometry of sulcal lines on the brain

Bases of Algorithms in Riemannian Manifolds

Riemannian metric :

- Dot product on tangent space
- Speed, length of a curve
- Shortest path: Riemannian Distance
- Geodesics characterized by 2nd order diff eqs: **locally unique for initial point and speed**

Exponential map (Normal coord. syst.) :

- Geodesic shooting: $Exp_x(v) = \gamma_{(x,v)}(1)$
- Log: find vector to shoot right (geodesic completeness!)

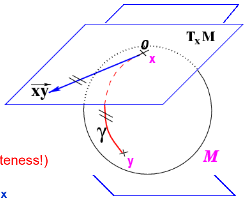

Reformulate algorithms with $\exp_x$ and $\log_x$

- Vector -> Bipoint (no more equivalent class)

Operator	Euclidean space	Riemannian manifold
Subtraction	$\overrightarrow{xy} = y - x$	$\overrightarrow{xy} = Log_x(y)$
Addition	$y = x + \overrightarrow{xy}$	$y = Exp_x(\overrightarrow{xy})$
Distance	$\mathrm{dist}(x,y) = \|y - x\|$	$\mathrm{dist}(x,y) = \|\overrightarrow{xy}\|_x$
Gradient descent	$x_{t+\varepsilon} = x_t - \varepsilon \nabla C(x_t)$	$x_{t+\varepsilon} = Exp_{x_t}(-\varepsilon \nabla C(x_t))$

Fréchet expectation (1944)

Minimizing the variance $\quad \mathrm{E}[\mathbf{x}] = \underset{y \in \mathrm{M}}{\mathrm{argmin}} \left(\mathrm{E}\left[\mathrm{dist}(y, \mathbf{x})^2\right] \right)$

Existence

- Finite variance at one point

Characterization as an exponential barycenter (P(C)=0)

$$\mathrm{grad}\left(\sigma_{\mathbf{x}}^2(y)\right) = 0 \quad \Rightarrow \quad \mathrm{E}\left[\overrightarrow{\bar{x}\mathbf{x}}\right] = \int_{\mathrm{M}} \overrightarrow{\bar{x}\mathbf{x}}.\, p_{\mathbf{x}}(z).d\mathrm{M}(z) = 0$$

Uniqueness Karcher 77 / Kendall 90 / Afsari 10 / Le 10

- Unique Karcher mean (thus Fréchet) if distribution has support in a regular geodesic ball with radius $r < r^* = \frac{1}{2}\min(inj(M), \pi/\sqrt{\kappa})$ (k upper bound on sectional curvatures on M)

Other central primitives $\quad \mathrm{E}^{\alpha}[\mathbf{x}] = \underset{y \in \mathrm{M}}{\mathrm{argmin}} \left(\mathrm{E}\left[\mathrm{dist}(y, \mathbf{x})^{\alpha}\right] \right)^{1/\alpha}$

First Statistical Tools: Moments

Gauss-Newton Geodesic marching

$$\bar{x}_{t+1} = \exp_{\bar{x}_t}(\tau\, v) \quad \text{with} \quad v = \mathrm{E}[\overrightarrow{y\mathbf{x}}] = \frac{1}{n}\sum_{i=1}^{n} \mathrm{Log}_{\bar{x}_t}(\mathrm{x}_i)$$

Covariance (PCA) [higher moments]

$$\Sigma_{\mathbf{xx}} = \mathrm{E}\left[\left(\overrightarrow{\bar{x}\mathbf{x}}\right).\left(\overrightarrow{\bar{x}\mathbf{x}}\right)^{\mathrm{T}}\right] = \int_{\mathrm{M}} \left(\overrightarrow{\bar{x}z}\right).\left(\overrightarrow{\bar{x}z}\right)^{\mathrm{T}}.\, p_{\mathbf{x}}(z).\, d\mathrm{M}(z)$$

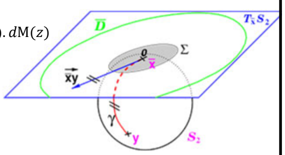

Principal component analysis

- Tangent-PCA:
  principal modes of the covariance
- Principal Geodesic Analysis (PGA) [Fletcher 2004,Sommer 2014]

[Oller & Corcuera 95, Battacharya & Patrangenaru 2002, Pennec, JMIV06, NSIP'99]

Computing on manifolds: a summary

The Riemannian metric easily gives

- Intrinsic measure and probability density functions
- Expectation of a function from M into R (variance, entropy)

Integral or sum in M: minimize an intrinsic functional

- Fréchet / Karcher mean: minimize the variance
- Filtering, convolution: weighted means
- Gaussian distribution: maximize the conditional entropy

The exponential chart corrects for the curvature at the reference point

- Gradient descent: geodesic walking
- Covariance and higher order moments
- Laplace Beltrami for free

[Pennec, NSIP'99, JMIV 2006, Pennec et al, IJCV 66(1) 2006, Arsigny, PhD 2006]

Course overview

Computing with tensor images

- Diffusion tensor imaging
- Statistical computing on manifolds
- An affine invariant Riemannian metric
- Interpolation, filtering, diffusion PDEs on Tensors
- Other metrics

Applications of manifold valued image processing

- Diffusion tensor imaging
- Morphometry of sulcal lines on the brain

GL(n)-Invariant Metrics on SPD matrices

Action of the Linear Group GL_n $A * \Sigma = A.\Sigma.A^T$

Invariant metric $\langle W_1 | W_2 \rangle_\Sigma = \langle A W_1 A^t | A W_2 A^t \rangle_{A\Sigma A^t} \overset{def}{=} \langle \Sigma^{-1/2} * W_1, \Sigma^{-1/2} * W_2 \rangle_{Id}$

- Isotropy group at the identity: Rotations
- All rotationally invariant scalar products:

$$\langle W_1 | W_2 \rangle_{Id} \overset{def}{=} \mathrm{Tr}\left(W_1^T W_2\right) + \beta\, \mathrm{Tr}(W_1).\mathrm{Tr}(W_2) \quad (\beta > \text{-}1/n)$$

- Geodesics at Id $\Gamma_{Id,W}(t) = \exp(tW)$
- Exponential map $Exp_\Sigma(\overrightarrow{\Sigma\Psi}) = \Sigma^{1/2} \exp(\Sigma^{-1/2}.\overrightarrow{\Sigma\Psi}.\Sigma^{-1/2})\Sigma^{1/2}$
- Log map $\overrightarrow{\Sigma\Psi} = Log_\Sigma(\Psi) = \Sigma^{1/2} \log(\Sigma^{-1/2}.\Psi.\Sigma^{-1/2})\Sigma^{1/2}$
- Distance $dist(\Sigma, \Psi)^2 = \langle \overrightarrow{\Sigma\Psi} | \overrightarrow{\Sigma\Psi} \rangle_\Sigma = \left\| \log(\Sigma^{-1/2}.\Psi.\Sigma^{-1/2}) \right\|_{Id}^2$

GL(n)-Invariant Metrics on Tensors

$$\|W\|_{\Sigma}^{2} = \mathrm{Tr}\left(W.\Sigma^{-1}W\Sigma^{-1}\right) + \beta\,\mathrm{Tr}\left(W\Sigma^{-1}\right)^{2} \quad (\beta > -1/n)$$

Space of Gaussian distributions (Information geometry) (β=0)
- Fisher information metric [Burbea & Rao J. Multivar Anal 12 1982, Skovgaard Scand J. Stat 11 1984, Calvo & Oller Stat & Dec. 9 1991]
- Tensor segmentation [Lenglet RR04 & JMIV 25(3) 2006]

Affine-invariant metrics for DTI processing (β=0)
- [Pennec, Fillard, Ayache, IJCV 66(1), Jan 2006 / INRIA RR-5255, 2004]
- PGA on tensors [Fletcher & Joshi CVMIA04, SigPro 87(2) 2007]

Geometric means (β=0)
- Covariance matrices in computer vision [Forstner TechReport 1999]
- Math. properties [Moakher SIAM J. Matrix Anal App 26(3) 2004]
- Geodesic Anisotropy [Batchelor MRM 53 2005]

Homogeneous Embedding (β=-1/(n+1))
- [Lovric & Min-Oo, J. Multivar Anal 74(1), 2000]

Course overview

Computing with tensor images
- Diffusion tensor imaging
- Statistical computing on manifolds
- An affine invariant Riemannian metric
- Interpolation, filtering, diffusion PDEs on Tensors
- Other metrics

Applications of manifold valued image processing
- Diffusion tensor imaging
- Morphometry of sulcal lines on the brain

Tensor interpolation

Geodesic walking in 1D

$\Sigma(t) = \exp_{\Sigma_1}(t\,\overrightarrow{\Sigma_1\Sigma_2})$

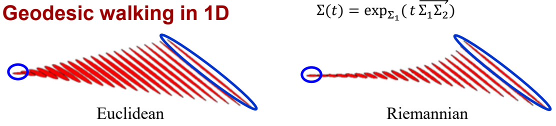

Bi-linear, tri-linear or spline interpolation? / **Rephrase as weighted mean**

$\Sigma(x) = \min_{\Sigma} \sum w_i(x)\ dist(\Sigma, \Sigma_i)^2$

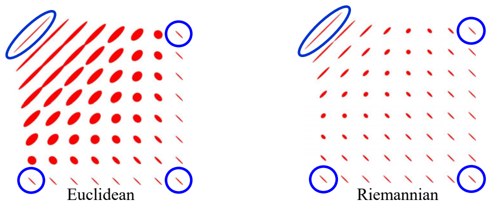

Gaussian filtering: Gaussian weighted mean

$$\Sigma(x) = \min \sum_{i=1}^{n} G_\sigma(x - x_i)\ dist\ (\Sigma, \Sigma_i)^2$$

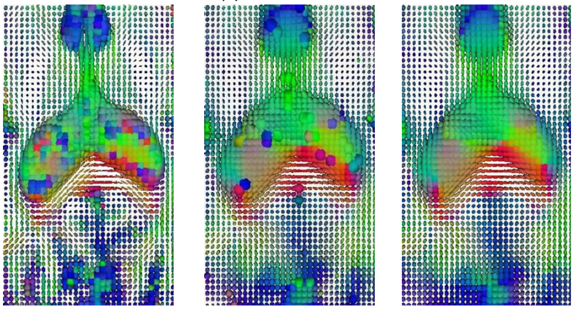

Raw | Coefficients σ=2 | Riemann σ=2

PDE for filtering and diffusion

Harmonic regularization $C(\Sigma) = \int_\Omega \|\nabla\Sigma(x)\|^2_{\Sigma(x)}\, dx$

- Gradient = manifold Laplacian

$$\Delta\Sigma(x) = \sum_{i=x,y,z} \partial_i^2\Sigma - \sum_{i=x,y,z} (\partial_i\Sigma)\Sigma^{(-1)}(\partial_i\Sigma) = \sum_u \frac{\overrightarrow{\Sigma(x)\Sigma(x+u)}}{\|u\|^2} + O(\|u\|^2)$$

- Trivial intrinsic numerical schemes with exponential maps!
- Geodesic marching $\Sigma_{t+1}(x) = \exp_{\Sigma_t(x)}(-\varepsilon\nabla C(\Sigma)(x))$

Anisotropic diffusion

- Perona-Malik 90 / Gerig 92 $\Delta_w\Sigma(x) = \sum_u w\left(\|\partial_u\Sigma(x)\|_{\Sigma(x)}\right)\Delta_u\Sigma(x)$
- Robust functions $\mathrm{Reg}(\Sigma) = \int \Phi\left(\|\nabla\Sigma(x)\|^2_{\Sigma(x)}\right) dx$

[Pennec, Fillard, Arsigny, IJCV 66(1), 2005, ISBI 2006]

Anisotropic filtering

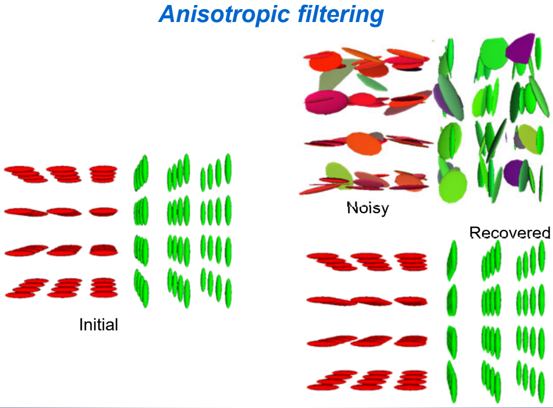

Anisotropic filtering

$$\hat{\Delta}\Sigma(x) = \sum_u w(\|\partial_u \Sigma(x)\|_{\Sigma(x)})\ \Delta_u \Sigma(x) \quad \text{with} \quad w(t) = \exp(-t^2/\kappa^2)$$

$$\Delta_u \Sigma(x) = \partial_u^2 \Sigma - (\partial_u \Sigma)\, \Sigma^{(-1)} (\partial_u \Sigma) \approx \overrightarrow{\Sigma(x)\Sigma(x+u)} / \|u\|^2$$

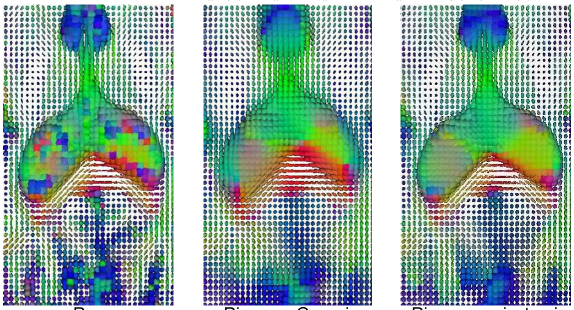

Raw | Riemann Gaussian | Riemann anisotropic

Extrapolation by Diffusion

$$C(\Sigma) = \frac{1}{2} \int_\Omega \sum_{i=1}^{n} G_\sigma(x - x_i) dist(\Sigma(x), \Sigma_i)^2 dx + \frac{\lambda}{2} \int_\Omega \|\nabla \Sigma(x)\|^2_{\Sigma(x)}$$

$$\nabla C(\Sigma)(x) = -\sum_{i=1}^{n} G_\sigma(x - x_i)\, \overrightarrow{\Sigma(x)\Sigma_i} - \lambda(\Delta\Sigma)(x)$$

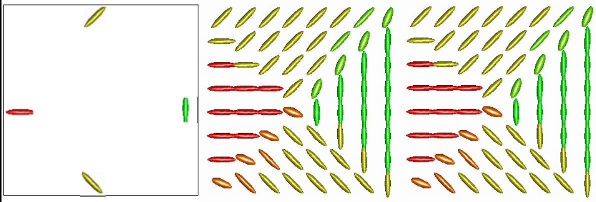

Original tensors | Diffusion λ=0.01 | Diffusion $\lambda=\infty$

Course overview

Computing with tensor images

- Diffusion tensor imaging
- Statistical computing on manifolds
- An affine invariant Riemannian metric
- Interpolation, filtering, diffusion PDEs on Tensors
- Other metrics

Applications of manifold valued image processing

- Diffusion tensor imaging
- Morphometry of sulcal lines on the brain

Log Euclidean Metric on Tensors

Exp/Log: global diffeomorphism Tensors/sym. matrices

- Carry vector space structure from tg space to manifold
  - Log. product
  - Log scalar product
  - Bi-invariant metric

$$\Sigma_1 \otimes \Sigma_2 \equiv \exp\left(\log(\Sigma_1) + \log(\Sigma_2)\right)$$

$$\alpha \bullet \Sigma \equiv \exp\left(\alpha \log(\Sigma)\right) = \Sigma^{\alpha}$$

$$dist\left(\Sigma_1, \Sigma_2\right)^2 \equiv \left\|\log\left(\Sigma_1\right) - \log\left(\Sigma_2\right)\right\|^2$$

Properties

- Invariance by the action of rotations + scale only
- Very simple algorithmic framework

[Arsigny, MICCAI 2005 & MRM 56(2), 2006]

Riemannian Frameworks on tensors

Affine-invariant Metric **(Curved space – Hadamard)**

- Dot product $\left\langle V \mid W \right\rangle_{\Sigma} = \left\langle AVA^T \mid AWA^T \right\rangle_{A\Sigma A^T} = \left\langle \Sigma^{-1/2} V \Sigma^{-1/2} \mid \Sigma^{-1/2} W \Sigma^{-1/2} \right\rangle_{Id}$
- Geodesics $Exp_{\Sigma}(t.\overrightarrow{\Sigma\Psi}) = \Sigma^{1/2} \exp(t.\Sigma^{-1/2}.\overrightarrow{\Sigma\Psi}.\Sigma^{-1/2})\Sigma^{1/2}$
- Distance $\mathrm{dist}(\Sigma, \Psi)^2 = \left\langle \overrightarrow{\Sigma\Psi} \mid \overrightarrow{\Sigma\Psi} \right\rangle_{\Sigma} = \left\| \log(\Sigma^{-1/2}.\Psi.\Sigma^{-1/2}) \right\|_{L_2}^2$

[Pennec, Fillard, Ayache, IJCV 66(1), 2006, Lenglet JMIV'06, etc]

Log-Euclidean similarity invariant metric **(vector space)**

- Transport Euclidean structure through matrix exponential
- Dot product $\left\langle V \mid W \right\rangle_{\Sigma} = \left\langle \partial_V \log(\Sigma) \mid \partial_W \log(\Sigma) \right\rangle_{Id}$
- Geodesics $Exp_{\Sigma}(t.\overrightarrow{\Sigma\Psi}) = \exp(\log(\Sigma) + t.\partial_{\overrightarrow{\Sigma\Psi}} \log(\Sigma))$
- Distance $\mathrm{dist}\left(\Sigma_1, \Sigma_2\right)^2 \equiv \left\|\log\left(\Sigma_1\right) - \log\left(\Sigma_2\right)\right\|^2$

[Arsigny, Pennec, Fillard, Ayache, SIAM'06, MRM'06]

Log Euclidean vs Affine invariant

- Means are geometric (vs arithmetic for Euclidean)
- Log Euclidean slightly more anisotropic
- Speedup ratio: 7 (aniso. filtering) to >50 (interp.)

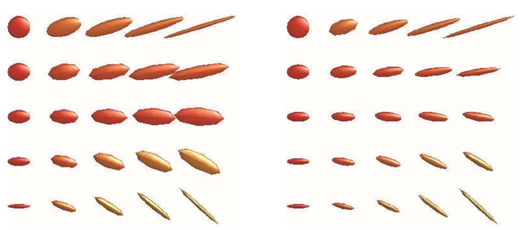

Euclidean Affine Log Euclidean

Log Euclidean vs Affine invariant

Real DTI images: anisotropic filtering

- Difference is not significant
- Speedup of a factor 7 for Log-Euclidean

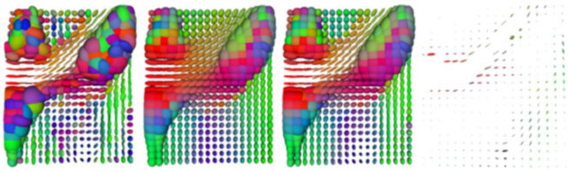

Original | Euclidean | Log-Euclidean | Diff. LE/affine (x100)

Some other metrics on tensors

Riemannian metrics

- Cholesky [Wang Vemuri et al, IPMI'03, TMI 23(8) 2004]
- Size and shape space [Dryden, Koloydenko & Zhou, 2008]
- Power Euclidean [Dryden & Pennec, arXiv 2011]
- Mixed-Power-Euclidean [Thanwerdas, XP DGA 2022]
- Alpha-Procrustes [HaQuang 2019]
- Polar-Affine [Su12], Bogoliubov-Kubo-Mori [Michor 2000]
- Bures-Wasserstein [Takatsu 2010, Bhatia 2019, Thanwerdas, XP 2023]
- Rotational vs Cholesky invariance [Thanwerdas, XP, LAA 2023]

Non Riemannian distances

- J-Divergence [Wang & Vemuri, TMI 24(10), 2005]
- Geodesic Loxodromes [Kindlmann et al. MICCAI 2007]

4th order tensors

- [Gosh, Descoteau & Deriche MICCAI'08]

Geodesic shooting in tensors spaces

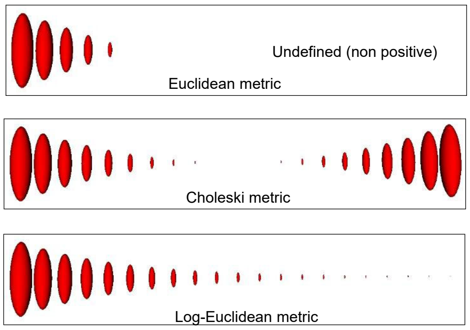

Course overview

Computing with tensor images

- Diffusion tensor imaging
- Statistical computing on manifolds
- An affine invariant Riemannian metric
- Interpolation, filtering, diffusion PDEs on Tensors
- Other metrics

Applications of manifold valued image processing

- Diffusion tensor imaging
- Morphometry of sulcal lines on the brain

DTI Estimation from DWI

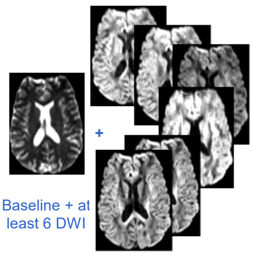

Baseline + at least 6 DWI

Stejskal & Tanner diffusion equation

$$S_i = S_0 \exp\left(-b g_i^T D g_i\right)$$

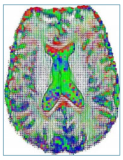

Diffusion Tensor Field

Noise is Gaussian in complex DW signal

- Rician = amplitude of complex Gaussian
- LSQ on Rician noise = bias for low SNRs [Sijbers, TMI 1998]

Estimation / Regularization on complex DWI:

- Anisotropic diffusion on Choleski factors [Wang & Vemuri, TMI'04]

Estimation with a Rician noise

- Smoothing DWI before estimation [Basu & Fletcher, MICCAI 2006]
- ML (MMSE) [Aja-Fernández et al, TMI 2008]
- MAP with log-Euclidean prior [Fillard et al., ISBI 2006, TMI 2007]

DTI Estimation from DWI

Maximum Likelihood Estimation

$$S_i = S_0 \exp\left(-b\, \mathbf{g}_i^T \Sigma\, \mathbf{g}_i\right) + Noise$$

- ML with Log-Gaussian noise:
  - linear system on the log-Images

$$\arg\min_D \sum_i \left(\log(S_i / S_0) + b g_i^T D g_i\right)^2$$

- ML with Gaussian noise on the MRIs:
  - non-linear optimization

$$\arg\min_D \sum_i \left(S_i - S_0 \exp(-b g_i^T D g_i)\right)^2$$

Actual MRI Noise

- Gaussian on the complex signal
- Rician on the amplitude

$$\hat{S}_i = \sqrt{(S_i + N_1(0,\sigma))^2 + N_2(0,\sigma)^2}$$

- This leads to a bias for low SNRs [Sijbers, TMI 1998]

$$E[\hat{S}_i] \approx E[S_i] + \frac{\sigma^2}{2S_i}$$

MAP Estimation with a Rician Noise Model

Maximum Likelihood estimator for Rician noise:

$$Sim(\Sigma) = -\sum_{i=1}^{N} \log\left(p(\hat{S}_i / S_i)\right) \qquad p(\hat{S}_i / S_i) = \frac{\hat{S}_i}{\sigma^2} \exp\left(-\frac{\hat{S}_i^2 + S_i(\Sigma)^2}{2\sigma^2}\right) I_0\left(\frac{S_i(\Sigma)\hat{S}_i}{\sigma^2}\right)$$

Anisotropic Log-Euclidean spatial prior

$$Reg(\Sigma) = \int \Phi\left(\|\nabla\Sigma(x)\|^2_{\Sigma(x)}\right) dx$$

Gradient descent in Log-Euclidean space

$$E(\Sigma) = \underbrace{Sim(\Sigma)}_{\text{Data fidelity term = ML}} + \lambda \underbrace{Reg(\Sigma)}_{\text{Smoothing term = prior}} \qquad \Sigma_{t+1} = Exp_{\Sigma_t}(-\varepsilon.\nabla E(\Sigma_t))$$

[Fillard, Arsigny, Pennec, Ayache ISBI'06, TMI 26(11) 2007]

37

Synthetic Data

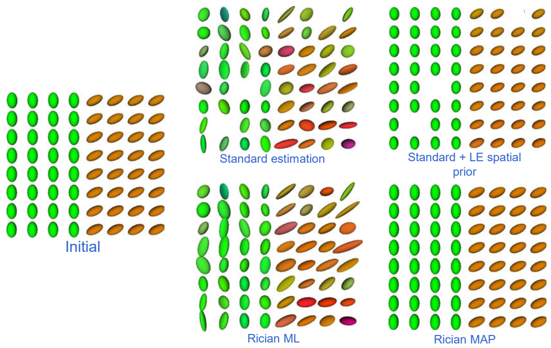

MVA 2024-2025 38

Rician MAP estimation with Riemannian spatial prior

$$MAP(\Sigma) = -\sum_{i=1}^{N} \int \log\left(\frac{\hat{S}_i}{\sigma^2} \exp\left(-\frac{\hat{S}_i^2 + S_i(\Sigma)^2}{2\sigma^2}\right) I_0\left(\frac{S_i(\Sigma)\hat{S}_i}{\sigma^2}\right)\right).dx + \int \Phi\left(\|\nabla\Sigma(x)\|^2_{\Sigma(x)}\right).dx$$

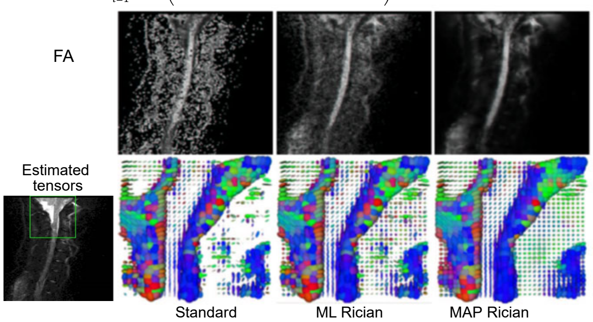

[Fillard, Arsigny, Pennec, Ayache ISBI'06, TMI 26(11) 2007]

MVA 2024-2025 39

Clinical DTI of the spinal cord: fiber tracking

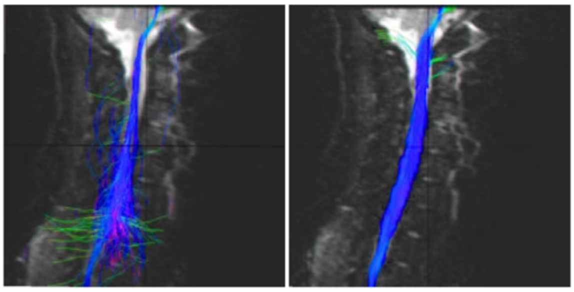

Standard MAP Rician

[Fillard, Arsigny, Pennec, Ayache ISBI'06, TMI 26(11) 2007]

Impact on fibers tracking

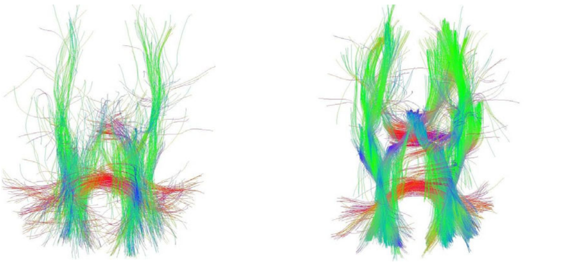

Euclidean interpolation Riemannian interpolation + anisotropic filtering

[Fillard, Toussaint et al, MedINRIA: DTI Processing and Visualization Software, 2006]

From images to anatomy

- Classify fibers into tracts (anatomo-functional architecture)?
- Compare fiber tracts between subjects?

Impact on fibers tracking

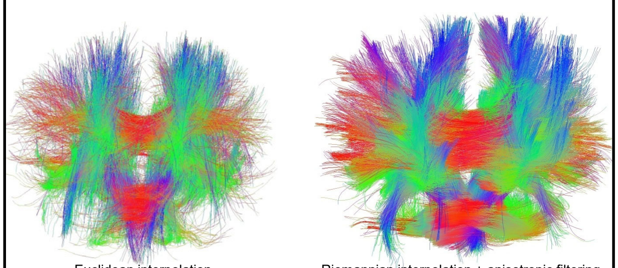

Euclidean interpolation Riemannian interpolation + anisotropic filtering

[Fillard, Toussaint et al, MedINRIA: DTI Processing and Visualization Software, 2006]

From images to anatomy

- Classify fibers into tracts (anatomo-functional architecture)?
- Compare fiber tracts between subjects?

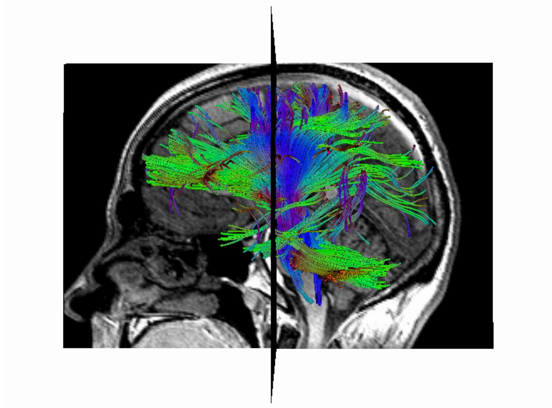

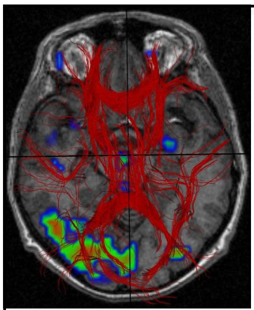

T1 + Activation map + fibers

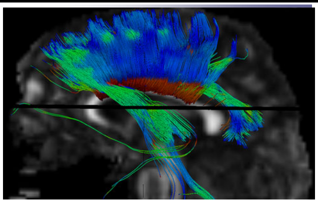

Corpus callosum + cingulum

Courtesy of P. Fillard using MedINRIA

Corticospinal tract and thalamo cortical connections

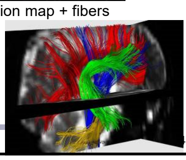

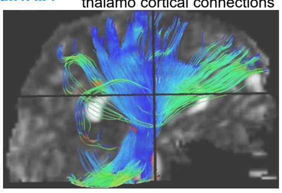

A Statistical Atlas of the Cardiac Fiber Structure

[J.M. Peyrat, et al., MICCAI'06, TMI 26(11), 2007]

Database

- 7 canine hearts from JHU
- Anatomical MRI and DTI

- *Average cardiac structure*
- Variability of fibers, sheets

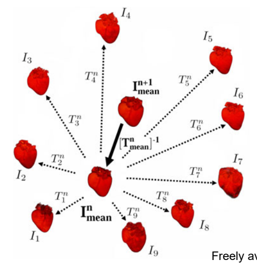

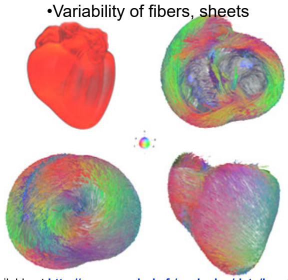

Freely available at http://www-sop.inria.fr/asclepios/data/heart

A Statistical Atlas of the Cardiac Fiber Structure

[J.M. Peyrat, et al., MICCAI'06, TMI 26(11), 2007]

Database

- 7 canine hearts from JHU
- Anatomical MRI and DTI

Method

- Normalization based on aMRIs
- Log-Euclidean statistics of Tensors

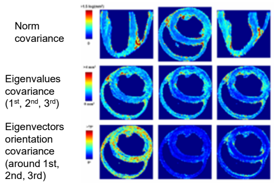

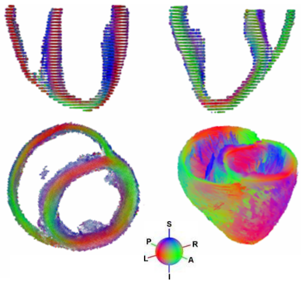

Diffusion model of the human heart

10 human ex vivo hearts (CREATIS-LRMN, Lyon, France)

- Classified as healthy (controlling weight, septal thickness, pathology examination)
- Acquired on 1.5T MR Avento Siemens
  - bipolar echo planar imaging, 4 repetitions, 12 gradients
- Volume size: 128×128×52, 2 mm resolution

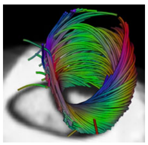

Fiber tractography in the left ventricle

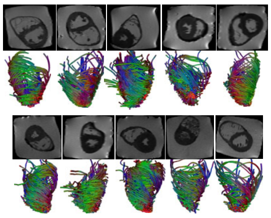

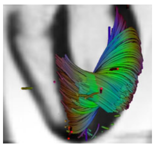

Helix angle highly correlated to the transmural distance

[H. Lombaert Statistical Analysis of the Human Cardiac Fiber Architecture from DT-MRI, ISMRM 2011, FIMH 2011]

A Statistical Atlas of the Cardiac Fiber Structure

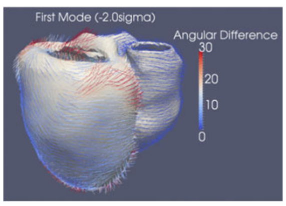

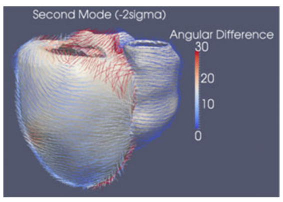

10 human ex vivo hearts (CREATIS-LRMN, France)

- Classified as healthy (controlling weight, septal thickness, pathology examination)
- Acquired on 1.5T MR Avento Siemens
  - bipolar echo planar imaging, 4 repetitions, 12 gradients
- Volume size: 128×128×52, 2 mm resolution

[R. Mollero, M.M Rohé, et al, FIMH 2015]

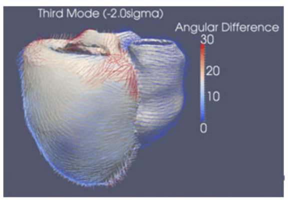

Course overview

Computing with tensor images
- Diffusion tensor imaging
- Statistical computing on manifolds
- An affine invariant Riemannian metric
- Interpolation, filtering, diffusion PDEs on Tensors
- Other metrics

Applications of manifold valued image processing
- Diffusion tensor imaging
- Morphometry of sulcal lines on the brain

Morphometry of the Cortex from Sucal Lines

Associated team Brain-Atlas (2001-2006)
- LONI (UCLA) : P. Thompson et al.
- ASCLEPIOS (INRIA): V. Arsigny, N. Ayache, P. Fillard, X. Pennec

Neuroanatomical reference:
- 72 sulcal lines manually extracted and labeled
- 700 subjects

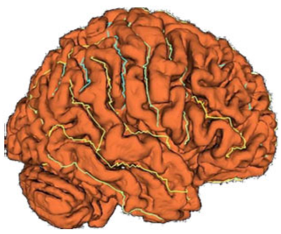

Alternative
- Automatic extraction

JF. Mangin, D. Rivière, 2003, SHFJ-CEA

Morphometry of the Cortex from Sucal Lines

Computation of the mean sulci: Alternate minimization of global variance
- Dynamic programming to match the mean to instances
- Gradient descent to compute the mean curve position

Extraction of the covariance tensors

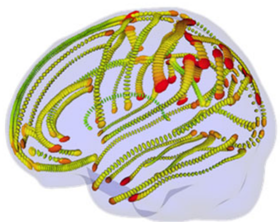

Currently:
80 instances of 72 sulci
About 1250 tensors

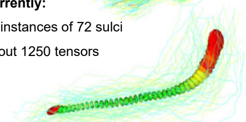

Covariance Tensors along Sylvius Fissure

Collaborative work between Asclepios (INRIA) Vand LONI (UCLA) P. Thompson
[Fillard et al IPMI05, LNCS 3565:27-38, NeuroImage 34(2):639-650, January 2007]

Compressed Tensor Representation

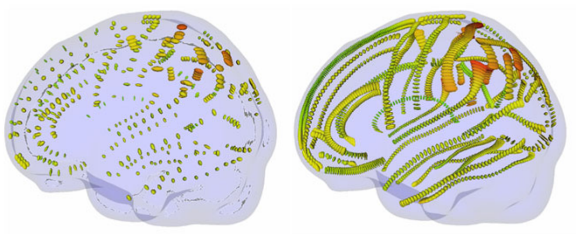

Representative Tensors (250)

Reconstructed Tensors (1250)
(Riemannian Interpolation)

Extrapolation by Diffusion

Minimize

$$C(\Sigma) = \frac{1}{2}\int_{\Omega} \sum_{i=1}^{n} G_\sigma(x - x_i) dist(\Sigma(x), \Sigma_i)^2 dx + \frac{\lambda}{2}\int_{\Omega} \|\nabla\Sigma(x)\|^2_{\Sigma(x)}\, dx$$

Evolution Equation : $\Sigma_{t+1}(x) = \exp_{\Sigma_t(x)}(-\varepsilon \nabla C(\Sigma)(x))$

$$\nabla C(\Sigma)(x) = -\sum_{i=1}^{n} G_\sigma(x - x_i)\, \overrightarrow{\Sigma(x)\Sigma_i} - \lambda(\Delta\Sigma)(x)$$

Extrapolation by Diffusion

$$C(\Sigma) = \frac{1}{2}\int_{\Omega} \sum_{i=1}^{n} G_\sigma(x - x_i) dist(\Sigma(x), \Sigma_i)^2 dx + \frac{\lambda}{2}\int_{\Omega} \|\nabla\Sigma(x)\|^2_{\Sigma(x)}$$

$$\nabla C(\Sigma)(x) = -\sum_{i=1}^{n} G_\sigma(x - x_i)\, \overrightarrow{\Sigma(x)\Sigma_i} - \lambda(\Delta\Sigma)(x)$$

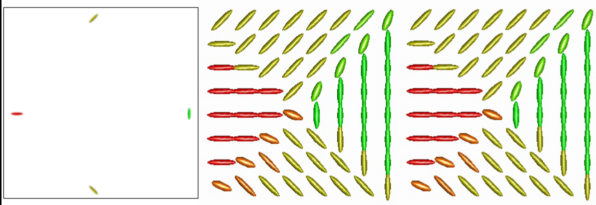

Original tensors Diffusion λ=0.01 Diffusion $\lambda=\infty$

Full Brain extrapolation of the variability

$$C(\Sigma) = \frac{1}{2}\int_{\Omega}\sum_{i=1}^{n} G_{\sigma}(x-x_i)\, dist(\Sigma(x),\Sigma_i)^2\, dx + \frac{\lambda}{2}\int_{\Omega}\|\nabla\Sigma\|^2_{\Sigma(x)}$$

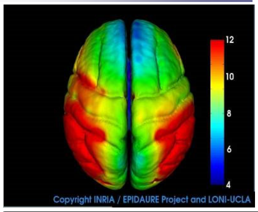

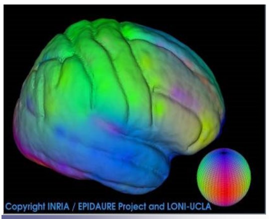

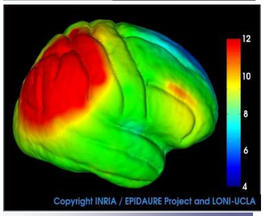

Comparison with cortical surface variability

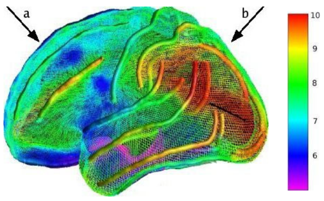

P. Thompson at al, HMIP, 2000

Average of 15 normal controls by non-linear registration of surfaces

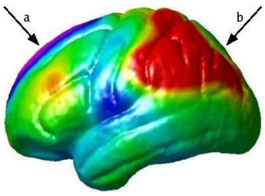

P. Fillard et al, IPMI 05

Extrapolation of our model estimated from 98 subjects with 72 sulci.

Consistent low variability in phylogenetical older areas

- (a) superior frontal gyrus

Consistent high variability in highly specialized and lateralized areas

- (b) temporo-parietal cortex

Quantitative Evaluation: Leave One Sulcus Out

- Remove data from one sulcus
- Reconstruct from extrapolation of others

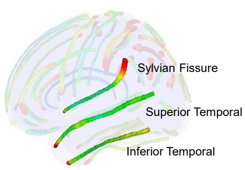

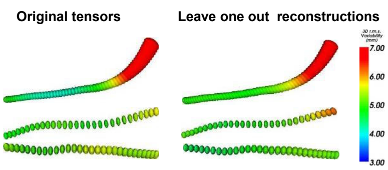

Asymmetry Measures

$$dist(\Sigma,\Sigma')^2 = \langle \overrightarrow{\Sigma\Sigma'} \mid \overrightarrow{\Sigma\Sigma'} \rangle_\Sigma = \left\| \log(\Sigma^{-1/2}.\Sigma'.\Sigma^{-1/2}) \right\|^2_{L_2}$$

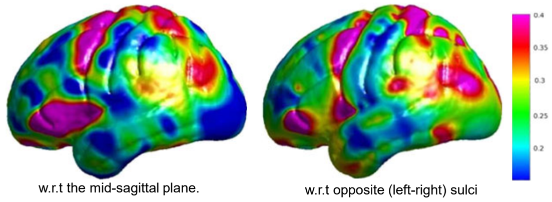

Greatest asymmetry	Lowest asymmetry
Broca's speech area and Wernicke's language comprehension area	Primary sensorimotor areas

Symmetry of the variability between groups

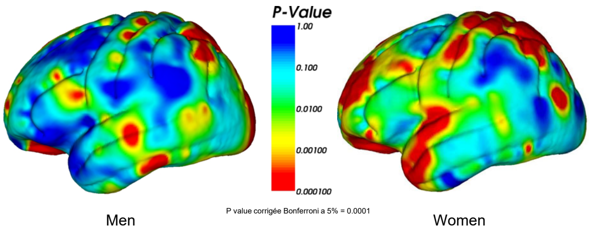

[Fillard, Pennec,Thompson, Thompson, Evaluating Brain Anatomical Correlations via Canonical Correlation Analysis of Sulcal Lines, MICCAI Workshop on stat. Atlases, 2007]

Local and distant structural correlation

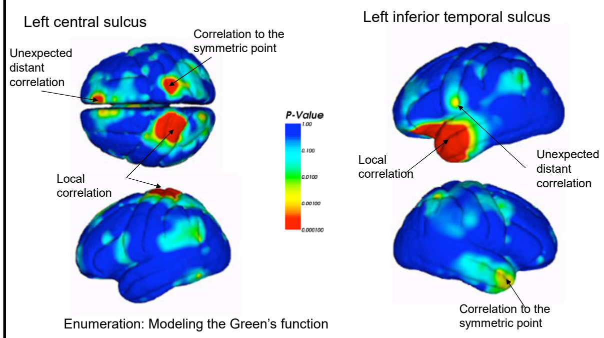

Enumeration: Modeling the Green's function

[Fillard, Pennec,Thompson, Thompson, Evaluating Brain Anatomical Correlations via Canonical Correlation Analysis of Sulcal Lines, MICCAI Workshop on stat. Atlases, 2007]